Pharmacological inhibition of casein kinase II attenuates metaflammation in a murine model of diet-induced metabolic dysfunction

ELISA PORCHIETTO[1*], ELEONORA AIMARETTI[2*], GIACOMO EINAUDI[1], GUSTAVO FERREIRA ALVES[1], DEBORA COLLOTTA[2], ENRICA MARZANI[2], LEONARDO CAMILLÒ[2], CHIARA RUBEO[3], RAFFAELLA MASTROCOLA[3], NATASHA IRRERA[4], MANUELA ARAGNO[3], CARLO CIFANI[1*] and MASSIMO COLLINO[2*]

[1]Pharmacology Unit, School of Pharmacy, University of Camerino, I-62032 Camerino, Italy; [2]Department of Neurosciences 'Rita Levi Montalcini', University of Turin, I-10125 Turin, Italy; [3]Department of Clinical and Biological Sciences, University of Turin, I-10125 Turin, Italy; [4]Department of Clinical and Experimental Medicine, University of Messina, I-98125 Messina, Italy

Received March 11, 2025; Accepted July 3, 2025

DOI: 10.3892/ijmm.2025.5616

Abstract. Kinases are activators of well-known inflammatory cascades implicated in metabolic disorders, and abnormal activation of casein kinase II (CK2) is associated with several inflammatory disorders. However, thus far, its role in the low-grade chronic inflammatory response known as 'metaflammation', which is a hallmark of obesity and type 2 diabetes, has not yet been elucidated. The present study aimed to evaluate the role of CK2 in diet-induced metaflammation and the effects of the CK2 inhibitor 4,5,6,7-tetrabromobenzotriazole (TBB) on a murine model fed a high-fat-high-sugar (HFHS) diet. C57BL/6JOlaHsd mice were fed a standard diet (n=12) or HFHS diet (n=24) for 12 weeks. A subgroup of the HFHS group received TBB (2.5 mg/kg/day, orally, n=12) for the last 8 weeks. Subsequently, plasma and liver samples were harvested for *ex vivo* biomolecular analyses (immunohistochemistry, western blotting, multiplex assay to determine the plasma levels of pro-inflammatory cytokines, reverse transcription-quantitative PCR and enzymatic assays) Statistical significance was determined using one-way ANOVA with post-hoc analysis ($P<0.05$). The results revealed that HFHS feeding induced glucose and lipid intolerance, elevated circulating pro-inflammatory cytokines and increased hepatic neutrophil infiltration. By contrast, TBB treatment improved glucose and lipid homeostasis, and reduced systemic inflammation without altering body weight. Notably, TBB attenuated hepatic inflammation, reduced neutrophil recruitment and suppressed HFHS-induced CK2α hyperactivation. This was accompanied by modulation of key inflammatory pathways, including NFκB/nucleotide-binding domain, leucine-rich-containing family, pyrin domain-containing-3 and AMPK signaling. In conclusion, the present study demonstrated the beneficial effects of pharmacological inhibition of CK2 in a murine model of diet-induced metabolic dysfunction, identifying CK2 as a potential target for dampening metaflammation. The efficacy of TBB in relieving hepatic inflammation was mainly due to the interference with selective inflammatory pathways.

Correspondence to: Professor Massimo Collino, Department of Neurosciences 'Rita Levi Montalcini', University of Turin, 30 Corso Raffaello, I-10125 Turin, Italy
E-mail: massimo.collino@unito.it

Abbreviations: ALT, alanine aminotransferase; AST, aspartate aminotransferase; CK2, casein kinase II; FASN, fatty acid nuclear synthase; FBP1, fructose-1,6-biphosphatase; HFHS, high-fat-high sugar; IR, insulin resistance; IκBα, inhibitor of κBα; ITT, insulin tolerance test; oGTT, oral glucose tolerance test; MPO, myeloperoxidase; NLRP3, nucleotide-binding domain, leucine-rich-containing family, pyrin domain-containing-3; SREBPs, sterol regulatory element-binding proteins; TBB, 4,5,6,7-tetrabromobenzotriazole

[*]Contributed equally

Key words: CK2, TBB, inflammation, HFHS diet

Introduction

Obesity, dyslipidemia and hyperinsulinemia are considered crucial metabolic risk factors affecting the onset of non-communicable diseases (1). A major driver of the high prevalence of these metabolic disorders is unhealthy dietary behavior, particularly the consumption of processed foods rich in saturated fats and simple sugars, but poor in fiber, minerals and vitamins; this dietary pattern is commonly referred to as the 'Western diet' (2,3). Evidence has indicated that low-grade chronic inflammation, also known as 'metaflammation', is a hallmark of diet-induced metabolic abnormalities, including obesity and insulin resistance (IR) (4,5). It is well established that the expansion of visceral adipose tissue due to overnutrition leads to tissue hypoxia, alterations in immune cell populations, such as macrophages and neutrophils, and

dysregulated cytokine production. These changes promote the release of pro-inflammatory cytokines, such as TNF-α, IL-6 and IL-1β, thereby contributing to the development of IR (6,7).

The association between IR and inflammation has been extensively explored during the last few decades, paving the way for the identification of several key contributors to this pathological condition. Specifically, kinases are among the most widely studied proteins acting as cross-talk mediators between metabolic inflammation and impaired insulin sensitivity. The activation of kinases is mediated by cytokine receptors and Toll-like receptors, and kinases themselves mediate the upregulation of signaling pathways, such as NFκB and MAPK cascades, leading to the release of cytokines, thus eliciting a feed-forward loop that exacerbates inflammation (8,9). Our previous study suggested that pharmacological targeting of these enzymes may offer therapeutic benefits for metabolic disorders; for example, selective inhibitors of JAKs, approved for treating rheumatoid arthritis and other chronic inflammatory conditions, have been shown to reduce body weight gain, improve glucose tolerance and alleviate IR in mice, alongside reducing both local and systemic inflammation (10). Similarly, JAK inhibition has been reported to improve glucose handling in fructose-induced diabetic rats (11).

The Ser/Thr kinase casein kinase II (CK2) is a ubiquitously expressed and constitutively active enzyme, structurally organized in a tetrameric form, composed of two catalytic (α and/or α') and two regulatory (β) subunits (12,13). CK2 directly phosphorylates several amino acid residues on some of the key factors involved in regulation of the NFκB cascade, including the inhibitor of κB α (IκBα) kinase (14-17) and the p65 subunit of NFκB (18,19), resulting in increased NFκB transcriptional activity and enhanced expression of downstream pro-inflammatory target genes (14,18).

Dysfunctional CK2 activity has been shown to be implicated in the onset of various pathological disturbances, thus indicating the need to determine its pleiotropic role as a master regulator of cell homeostasis. For example, elevated levels of CK2 have been reported in the serum of patients with type 2 diabetes (20), and increased activation of CK2 has been detected in murine white adipocytes, where it regulates energy expenditure (21), glucose homeostasis (22) and lipid metabolism (23).

Despite the growing body of evidence supporting the involvement of CK2 in metabolic disorders (21,23,24), the potential benefits of its pharmacological modulation in the context of diet-induced metabolic dysfunction remain poorly understood. To date, the effects of CK2 inhibition have been most convincingly demonstrated in adipocytes (24), where it markedly impacts the adipogenic program and the local regulation of fat metabolism. By contrast, limited data are available on the consequences of pharmacological CK2 inhibition in the liver, despite hepatic inflammation being a well-established contributor to both local and systemic impairments in glucose and lipid homeostasis (25). Notably, targeted genetic interventions in hepatic inflammatory pathways, such as the NFκB p65 subunit or pro-inflammatory kinases, including IκB kinase β and Rho-kinase 1, have been shown to markedly affect whole-body insulin sensitivity in mice subjected to a hypercaloric diet (26-28). The present study aimed to explore the effects of a CK2 ATP-competitive inhibitor, 4,5,6,7-tetrabromobenzotriazole (TBB), on molecular mechanisms driving hepatic inflammation and its potential association with changes in blood cytokines, as well as systemic markers of lipid and glucose profiles.

Materials and methods

Ethics statement. The *in vivo* experimental procedures performed in the present study were approved by the local Animal Use and Care Committee (University of Turin, Turin, Italy) and the Ministry of Health (approval no. 855/2021-PR), in keeping with the European Directive 2010/63/EU on the protection of animals used for scientific purposes, the Guide for the Care and Use of Laboratory Animals and ARRIVE guidelines (29-31).

Animal study and procedures. A total of 36 3-week-old male C57BL/6JOlaHsd mice (ENVIGO RMS SRL) were maintained in conventional housing conditions (n=5 mice/cage) in a controlled environment with a temperature of 25±2˚C and humidity of 45-65%, under an automatically controlled 12-h light/dark cycle, with *ad libitum* access to food and water. The basal body weight of the mice was 15-20 g, with no statistically significant differences among the groups. After 1 week of acclimatation, the mice were randomly divided into one of two dietary regimens: i) Fed a standard diet (SD; 3.85 kcal/g; cat. no. E157452-04; n=12), which provided 10% kcal from fat (soybean oil and lard), 70% kcal from carbohydrates (corn starch and maltodextrins) and 20% kcal from protein (Casein 30 Mesh and L-Cysteine); or ii) fed a high-fat-high-sugar (HFHS) diet (5.56 kcal/g; cat. no. E15772-34 ; n=24), which provided 58% kcal from fat (soybean oil and hydrogenated coconut oil) 25.5% kcal from carbohydrates (sucrose and maltodextrins), 16.4% kcal from protein (Casein 30 Mesh) and 0.1% kcal from micro-nutrients (including vitamins and minerals) for 12 weeks. Both diets were purchased from ssniff Spezialdiäten GmbH. The timing of the dietary intervention and the components of the diets were established according to previous experimental protocols that evoked IR, glucose intolerance and body weight gain in mice (32-34). After 4 weeks of dietary manipulation, a subgroup from the HFHS diet-fed mice received daily oral administration of TBB (CliniSciences) at the dosage of 2.5 mg/kg (HFHS + TBB; n=12). Sample size was calculated by G*Power 3.1™ software analysis (https://www.psychologie.hhu.de/arbeitsgruppen/allgemeine-psychologie-und-arbeitspsychologie/gpower; one-way ANOVA fixed effects, assuming an α of 0.05 and 80% power), based on previously published data recorded on serum TNF-α levels in a similar mouse model of diet-induced metabolic dysfunction (10). The dose was determined according to previous *in vivo* studies (35-37). Body weight and food intake were recorded weekly with a precision balance (VWR International S.r.l.). All reagents were purchased from MilliporeSigma unless otherwise stated.

Oral glucose tolerance test (oGTT) and insulin tolerance test (ITT). For the oGTT, after an overnight fast, blood glucose levels were measured with Accu-check Aviva glucometer (Roche Diabetes Care Italy S.P.A.). Next, a 30% D-glucose solution (2 g/kg) was administered orally, and glycaemia

was measured, specifically after 15, 30, 60 and 120 min. The ITT test was performed after 6 h of fasting; briefly, insulin (0.75 UI/kg) was injected intraperitoneally and glycaemia was measured 0, 15, 45, 60 and 90 min after the injection. Blood glucose levels were measured using a standard handheld glucometer requiring only 0.5 μl blood per sample. Tail vein sampling was conducted following a low-burden microsampling protocol, recognized in international guidelines (38-41), using a single puncture site and collecting <5 μl per sample, well below the established microsampling volume threshold.

Plasma and liver collection. At the end of the experimental protocol, after an overnight fast, mice were anesthetized with isoflurane (3%), delivered in oxygen (0.4 l/min flow rate) and blood was collected by cardiac exsanguination into vials containing EDTA (17 μM/ml). The blood samples were then centrifuged at 13,000 x g for 10 min at room temperature to obtain the plasma fraction. After cardiac exsanguination, the mice underwent cervical dislocation and liver samples were harvested, snap frozen in liquid nitrogen and stored at -80˚C. A portion of the hepatic tissue was cryoprotected in optimal cutting temperature compound, frozen in liquid nitrogen and stored at -80˚C for immunohistochemistry analysis.

Plasma analysis. Plasma levels of aspartate aminotransferase (AST; cat. no. CL36-275), alanine aminotransferase (ALT; cat. no. CL38-275), triglycerides (cat. no. CL53-200S) and total cholesterol (cat. no. CL21-200S) were measured using colorimetric clinical assay kits (FAR S.r.l.) according to the manufacturer's instructions. TNF-α, IL-1β, IL-6, IFN-γ and IL-17A plasma levels were measured using the Bio-Plex Pro™ Mouse Cytokine Th17 Panel A 6-Plex (cat. no. M6000007NY; Bio-Rad Laboratories, Inc.), according to the manufacturer's instructions.

Histological evaluation of hepatic inflammation with hematoxylin and eosin (H&E) staining. H&E staining was performed to evaluate the hepatic inflammatory infiltrates. Frozen liver tissues were cut into cryostatic sections (10 μm) and fixed in cold acetone for 2 min. Subsequently, the sections were rinsed in distilled water and incubated in Mayer's hematoxylin for 5 min at room temperature. The sections were then rinsed in tap water for 5 min and were counterstained with eosin solution for 1 min, followed by a brief wash in distilled water at room temperature. Finally, the sections were dehydrated in ascending ethanol solutions (70, 90 and 100%; 1 min/step), fixed in xylene solution for 1 min at room temperature and were mounted with DPX medium (MilliporeSigma) and coverslips. The stained tissues were viewed under a Zeiss Airyscan confocal microscope (magnification, x10 and x20; Zeiss GmbH). Images were analyzed utilizing ImageJ 1.54p (National Institutes of Health) to semi-quantify the inflammatory area as previously described (42).

Myeloperoxidase (MPO) activity assay. MPO activity assay was performed as previously described (43). Briefly, ~100 mg liver sections were homogenized in 20 mM PBS (pH=7.4) and centrifuged at 13,000 x g for 10 min at 4˚C. Pellets were then resuspended in 0.5 ml 0.5% hexadecyltrimethylammonium bromide in PBS (50 mM; pH 6) and centrifuged at 13,000 x g for 10 min at 4˚C. MPO activity was assessed by indirectly measuring the H_2O_2-dependent oxidation of 3,3',5,5'-tetramethylbenzidine dihydrochloride hydrate with a spectrophotometer (EnSight™; PerkinElmer, Inc.). Data are presented as optical density at 650 nm/mg of protein.

Immunohistochemistry. Immunohistochemical analysis was performed on the 10-μm liver cryostatic sections, which were fixed for 2 min in cold acetone. A solution of 1% Tween in PBS was used for 5 min at room temperature for permeabilization. After blocking with 3% bovine serum albumin (BSA; MilliporeSigma) in PBS at room temperature, the sections were incubated for 2 h at room temperature with an MPO primary antibody (1:30; cat. no. ab9535; Abcam) and were subsequently incubated for 45 min with horseradish peroxidase (HRP)-conjugated secondary antibodies at room temperature (1:400; cat. no. 7074; Cell Signaling Technology, Inc.). Chromogenic detection was assessed by exposing slides to DAB for 2 min and by counterstaining them with Mayer's hematoxylin for 5 min at room temperature. Stained tissues were viewed under a Zeiss Airyscan confocal microscope (magnification, x10 and x20). ImageJ 1.54p was used to semi-quantify the mean positive MPO area on x20 magnification images (n=3-4/group).

Western blot analysis. Total and cytosolic/nuclear liver protein extracts were prepared as previously described (44), and were quantified using the BCA protein assay (cat. nos. 23225 and 23250; Pierce; Thermo Fisher Scientific, Inc.). Briefly, 50 μg proteins were separated by SDS-PAGE on 8, 10 and 12% acrylamide gels, and were transferred to polyvinylidene difluoride membranes (cat. no. GE10600038; Merck KGaA) or nitrocellulose membranes (cat. no. GVS1215471; GVS S.p.a.). After 1 h of blocking with 10% BSA solution, the membranes were incubated at 4˚C overnight with the following primary antibodies: Rabbit anti-phosphorylated (p)-CK2α $pTyr^{255}$ (1:1,000; cat. no. SAB4504299; Merck KGaA) rabbit anti-total CK2α (1:1,000; cat. no. ab76040; Abcam), mouse anti-$Ser^{32/36}$ IκBα (1:1,000, cat. no. 9246), rabbit anti-total IκBα (1:1,000; cat. no. 9242), rabbit anti-total p65 NFκB (1:500; cat. no. 8242) (all from Cell Signaling Technology, Inc.), mouse anti-nucleotide-binding domain, leucine-rich-containing family, pyrin domain-containing-3 (NLRP3; 1:1,000; cat. no. AG-20B-0014-C100; AdipoGen Life Sciences), rabbit anti-cleaved caspase-1 (1:500; cat. no. 89332; Cell Signaling Technology, Inc.), mouse anti-total caspase 1 (1:1,000; cat. no. MA5-16215; Thermo Fisher Scientific, Inc.), rabbit anti-p-AMPK (1:1,000; cat. no. 2531), rabbit anti-total AMPK (1:1,000; cat. no. 2532), rabbit mouse anti-β-actin (1:1,000; cat. no. 4970) (all from Cell Signaling Technology, Inc.), goat anti-intercellular adhesion molecule 1 (ICAM-1; 1:1,000; cat. no. sc-1511), mouse anti-vinculin (1:1,000; cat. no. sc-73614) and mouse anti-proliferating cell nuclear antigen (PCNA; 1:1,000; cat. no. sc-25280) (all from Santa Cruz Biotechnology, Inc.). Subsequently, the blots were incubated with HRP-conjugated secondary antibodies at room temperature for 1 h (1:10,000; anti-mouse cat. no. 7076, anti-rabbit cat. no. 7074; both from Cell Signaling Technology, Inc.; anti-goat cat. no. 1721034; Bio-Rad Laboratories, Inc.). Proteins were detected with Clarity and Clarity Max Detection Kits (cat. nos. 1705061

and 1705062; Bio-Rad Laboratories, Inc.) and were semi-quantified using ImageLab Version 6.1.0 (Bio-Rad Laboratories, Inc.) and ImageJ software [ImageJ 1.54 h; Java1.8.0_345(64 bit)]. The results were normalized to the densitometric value of β-actin or vinculin for cytosolic and total proteins, and mouse PCNA for nuclear proteins. Housekeeping proteins were selected based on previously published papers supporting their stability and appropriateness in similar experimental settings (10,44-48). Semi-quantitative results of the p-proteins were shown as the ratio of the p-protein isoform to total protein expression. All values were expressed as fold change compared with SD-fed mice values.

Reverse transcription-quantitative PCR (qPCR). Total RNA was extracted from liver samples (15 mg) using Animal Tissue RNA Purification Kit (cat. no. 25700; Norgen Biotek Corp.), according to the manufacturer's instructions. RNA concentration was assessed using a NanoDropOne instrument (Thermo Fisher Scientific, Inc.) and 200 ng was reverse transcribed using SensiFAST™ cDNA Synthesis Kit 50 reactions (cat. no. BIO-65053; Meridian Bioscience) according to the manufacturer's instructions. qPCR was performed on 1 μl cDNA using the SensiFAST™ SYBR® No-ROX Kit (cat. no. BIO-98005; Meridian Bioscience) according to manufacturer's instructions. qPCR was conducted on the CFX Connect Real-Time PCR Detection System (Bio-Rad Laboratories, Inc.). The thermocycling conditions were as follows: 2 min at 95˚C for polymerase activation, followed by 40 cycles of 5 sec at 95˚C for denaturation, 10 sec at 55˚C for annealing and 13 sec at 72˚C for extension. Relative gene expression was obtained after normalization to the housekeeping gene GAPDH (cat. no. QT01658692; Mm_Gapdh_3_SG; Qiagen, Inc.), or 18S, using the formula $2^{-\Delta\Delta Cq}$ as previously described (49). Fold change was determined by comparison to the SD group. Forward and reverse sequences for TNF-α, IL-1β, IL-6, fatty acid nuclear synthase (FASN), sterol regulatory element-binding protein (SREBP)1c and 18S are listed in Table I and were purchased from biomers.net GmbH and from metabion international AG.

Table I. Primer sequences used for reverse transcription-quantitative PCR.

Gene	Primer sequence, 5'-3'
Forward TNF-α	GCAGTTTCTGTCCCTTTCAC
Reverse TNF-α	CATTTGGGAACTTCTCATCCCT
Forward IL-1β	CTTTGAAGAGCCCATCCT
Reverse IL-1β	CCGTCTTTCATTACACAGGACAG
Forward IL-6	CTGATGCTGGTGACAACCAC
Reverse IL-6	TCCACGATTTCCCAGAGAAC
Forward 18S	TGCGAGTACTCAACACCAACA
Reverse 18S	CTGCTTTCCTCAACACCACA
Forward SREBP1c	TGGAATCTAGCCCAGCCAGC
Reverse SREBP1c	AGACTGGTACGGGCCACAAG
Forward FASN	ACAGGAGTTCTGGGCCAACC
Reverse FASN	AGGAGGCGTCGAACTTGGAG

FASN, fatty acid nuclear synthase; SREBP1c, sterol regulatory element-binding protein 1c.

Statistical analysis. Data are presented as the mean ± SEM and 'n' indicates the number of mice studied. Graph-Pad Prism software version 7.05 (Dotmatics) was used for data analysis. Shapiro-Wilk test was adopted to assess the normality of the variable distributions and Bartlett's test was applied for establishing the homogeneity of the variances. Logarithmic transformation was applied to the data to ensure normality and homogeneity of variance, when necessary. One-way ANOVA followed by Bonferroni's test was used to assess normally distributed data. Non-parametric Kruskal-Wallis test followed by Dunn's post hoc analysis was employed for data that were not normally distributed or exhibited a heterogeneity of variance despite the logarithmic transformation. $P<0.05$ was considered to indicate a statistically significant difference.

Results

TBB administration counteracts diet-induced impairments in glucose and lipid profiles. As reported in Table II, HFHS diet-fed mice exhibited higher body weight gain compared with those fed an SD, due to the increase in total caloric intake, which was not reverted by TBB administration. Notably, no significant differences in food intake (g/day) were recorded among any of the experimental groups. HFHS diet-fed mice displayed altered glycemic and lipid profiles when compared with SD-fed mice, with higher fasting blood glucose levels and impaired glucose and insulin tolerance. Notably, TBB administration reduced both lipid levels and fasting blood glucose compared with those in the HFHS group, without significant effects on glucose handling capability, when recorded after the glucose challenge.

TBB administration protects against diet-induced liver injury. A significant increase was documented in the plasma levels of ALT and AST in the HFHS group compared with those in SD-fed mice (Fig. 1A and B), which was reversed by TBB administration, suggesting that chronic pharmacological treatment did not alter hepatic functionality and, most notably, was helpful in alleviating diet-induced hepatic injury. The deleterious impact of dietary manipulation on the liver was confirmed by the H&E staining (Fig. 1C), showing a significant increase in the area of inflammatory cells in the liver from HFHS diet-fed mice compared with that in the SD group, which was markedly reduced following TBB treatment (Fig. 1D). The HFHS diet-induced increase in hepatic infiltration of inflammatory cells was further supported by the detection of an upregulation of the adhesion molecule ICAM-1 (Fig. 2A), and a significant increase in the expression and activity of MPO, a well-known biomarker of leukocyte infiltration and lipid peroxidation (50) (Fig. 2B-D), in the liver of HFHS diet-fed mice when compared with SD-fed mice. Both the upregulation of ICAM-1, and the increased expression and activity of MPO, caused by chronic exposure to a hypercaloric diet, were markedly reduced when HFHS diet-fed mice were exposed to TBB.

Table II. Metabolic parameters assessed at the end of the protocol.

Parameter	SD	HFHS	HFHS + TBB
Body weight, g	27.89±0.46	44.32±0.82[a]	42.44±0.97[a]
Food intake, g/mouse/day	2.89±0.05	3.12±0.09	3.04±0.12
Fasting blood glucose, mg/dl	104.40±6.06	155.00±5.96[a]	130.4±5.12[a,b]
oGTT AUC, mg/dl x min x1,000	18.14±1.12	26.27±0.86[a]	25.30±1.04[a]
ITT AUC, mg/dl x min x1,000	4.75±0.15	7.85±0.20[a]	7.95±0.27[a]
Total cholesterol, mg/dl	66.33±5.41	212.30±13.29[a]	155.90±18.98[a,b]
Triglycerides, mg/dl	22.11±1.36	57.88±2.55[a]	27.23±1.79[a,b]

AUC, area under the curve; ITT, insulin tolerance test; HFHS, high-fat high-sugar; oGTT, oral glucose tolerance test; SD, standard diet; TBB, 4,5,6,7-tetrabromobenzotriazole. Data are presented as the mean ± SEM (n=12 mice/group). Statistical analysis was performed using one-way ANOVA followed by Bonferroni's post hoc test, [a]P<0.05 vs. SD; [b]P<0.05 vs. HFHS.

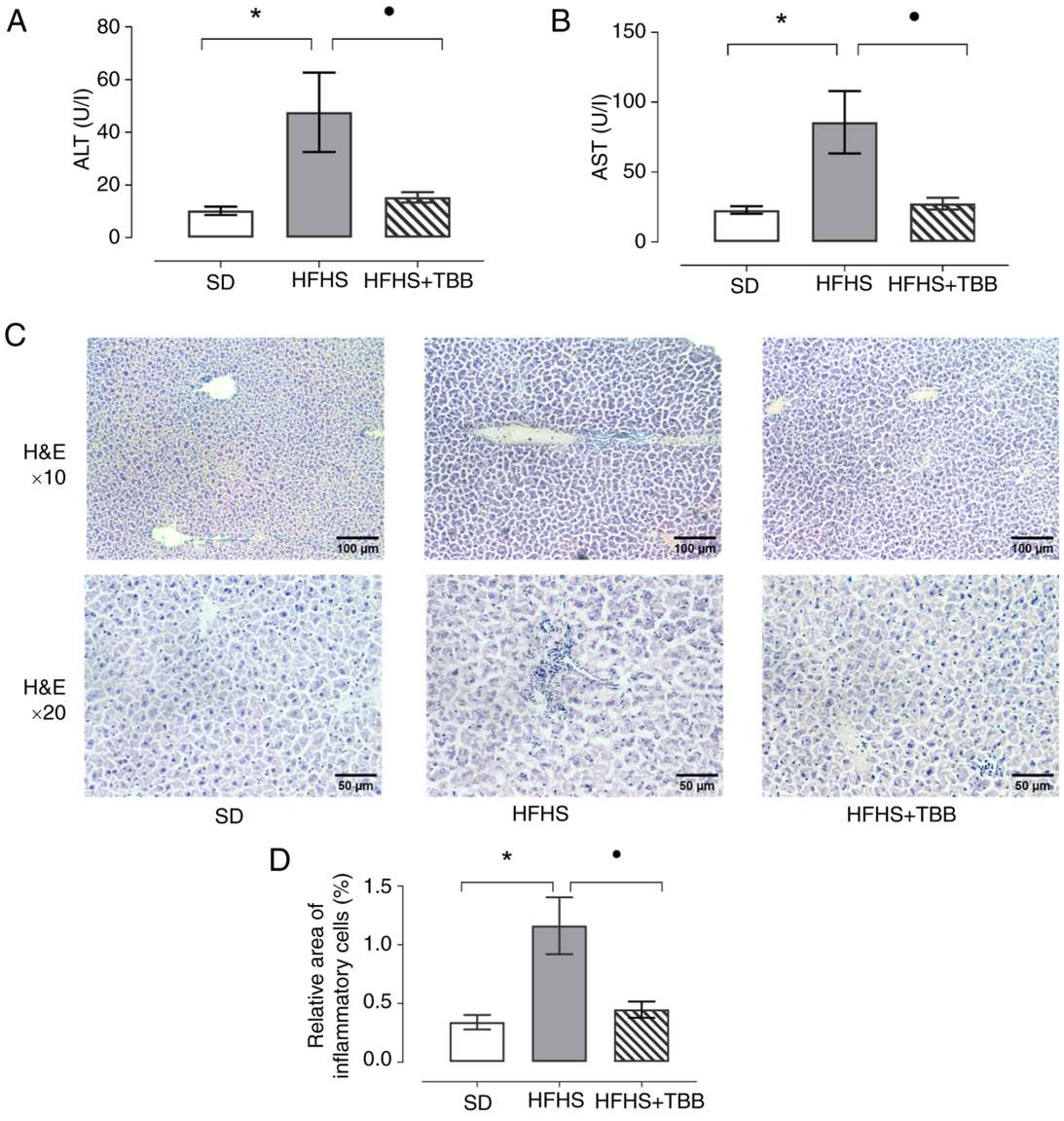

Figure 1. Effects of hypercaloric diet consumption and casein kinase II inhibition on hepatic inflammatory status. (A) ALT and (B) AST were measured in plasma samples using commercially available kits. Data are presented as the mean ± SEM (n=12 mice/group). Statistical analysis was performed by one-way ANOVA followed by Bonferroni's post hoc test for ALT, whereas AST was analyzed by Kruskal-Wallis followed by Dunn's post hoc test. (C) H&E staining was performed on hepatic cryopreserved tissues (n=5 mice/group). Representative photomicrographs of were recorded with a Zeiss Airyscan confocal microscope at (magnification, x10 and x20). (D) Relative area of inflammatory cells. Data are presented as the mean ± SEM (n=5 mice/group). Statistical analysis was performed by one-way ANOVA followed by Bonferroni's post hoc test. *P<0.05 vs. SD; •P<0.05 vs. HFHS. ALT, alanine aminotransferase; AST, aspartate aminotransferase; H&E. hematoxylin and eosin; HFHS, high-fat high-sugar; SD, standard diet; TBB, 4,5,6,7-tetrabromobenzotriazole.

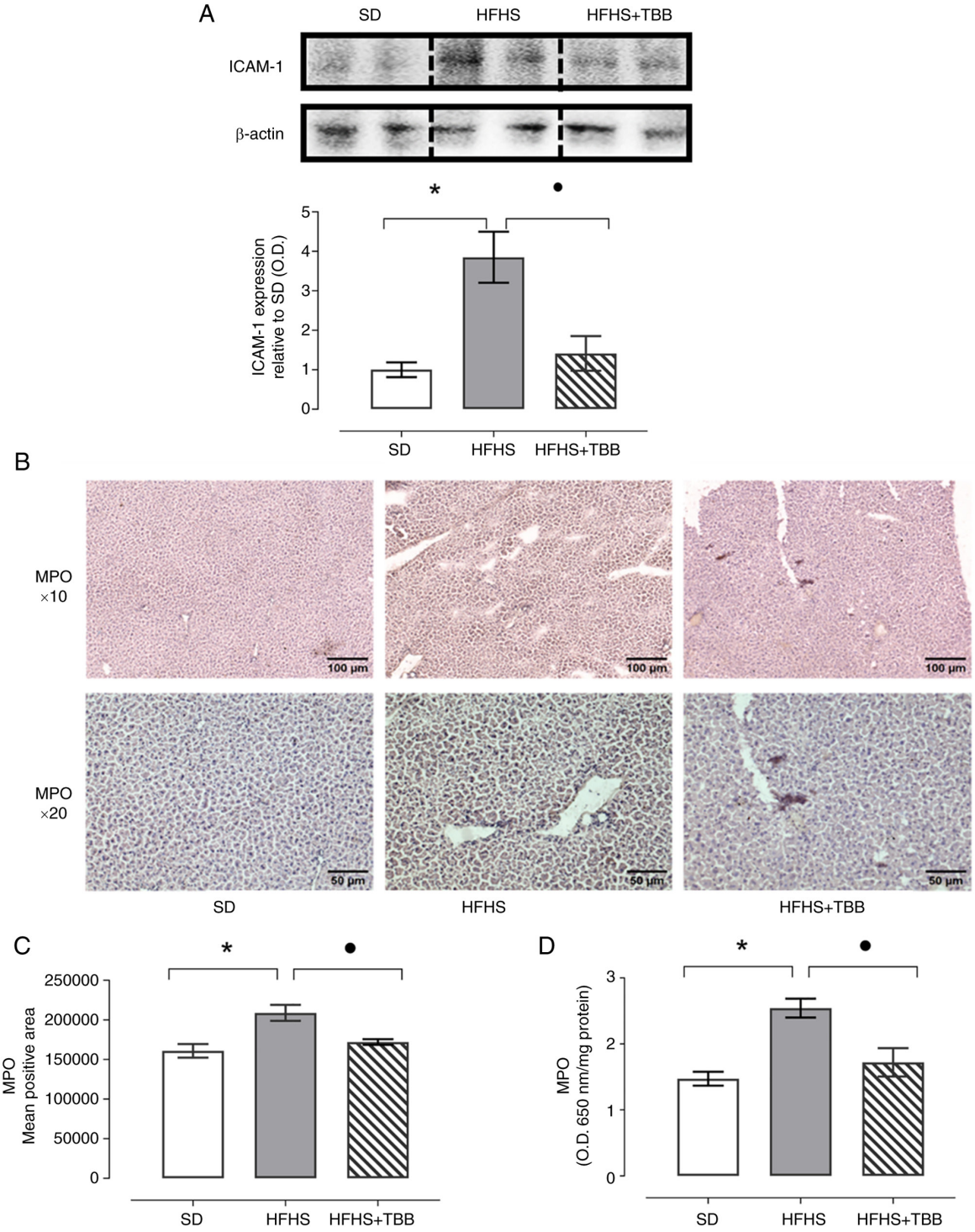

Figure 2. Assessment of ICAM-1 expression and neutrophilic recruitment at the hepatic level among the experimental groups. (A) Western blot analysis of ICAM-1 normalized to β-actin. Densitometric analysis of the bands is expressed as relative O.D. Data are presented as the mean ± SEM (n=4-5 mice/group). (B) Representative photomicrographs of MPO immunostaining were recorded (n=5 mice/group). Stained tissues were viewed under a Zeiss Airyscan confocal microscope (magnification, x10 and 20x). (C) Mean positive MPO area on x20 magnification images (n=3-4 mice/group). Data are presented as the mean ± SEM (n=3/4 mice per group). (D) MPO activity was measured using an *in vitro* assay. Data are presented as the mean ± SEM (n=10 mice/group). Statistical analysis was performed by one-way ANOVA followed by Bonferroni's post hoc test. *P<0.05 vs. SD; •P<0.05 vs. HFHS. HFHS, high-fat high-sugar; ICAM-1, intercellular adhesion molecule 1; MPO, myeloperoxidase; O.D., optical density; SD, standard diet; TBB, 4,5,6,7-tetrabromobenzotriazole.

TBB administration ameliorates AMPK phosphorylation and reduces the activation of pro-inflammatory signaling pathways in mice fed a HFHS diet. As shown by western blot analysis, HFHS diet-fed mice showed a statistically significant increase in the phosphorylation, and thus activation, of IκBα on $Ser^{32/36}$, compared with that in the SD group (Fig. 3A). This effect was paralleled by an increased nuclear translocation of the NFκB p65 subunit when compared with the SD group (Fig. 3B). Pharmacological intervention with TBB evoked a significant reduction in IκBα phosphorylation status as well

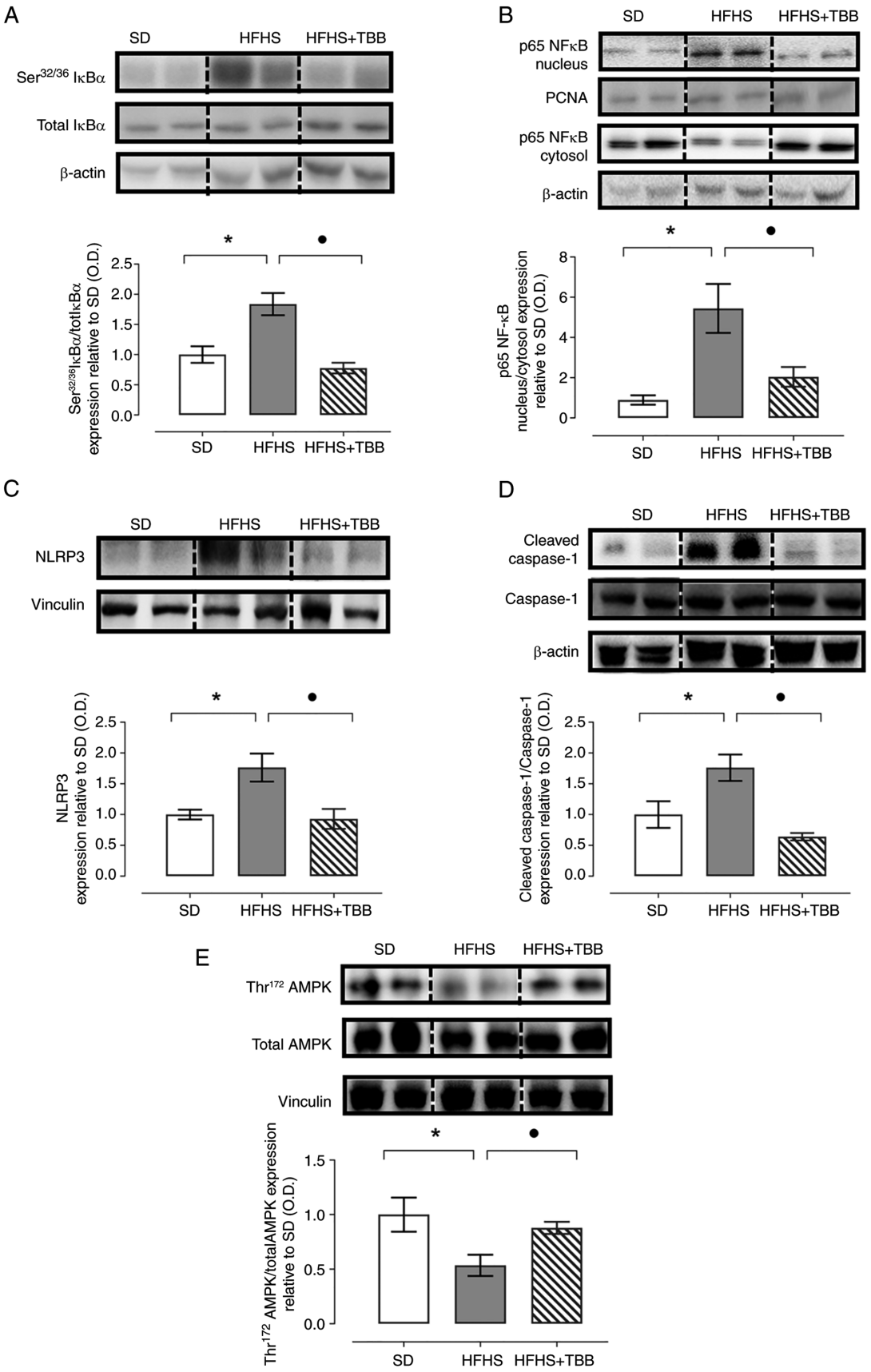

Figure 3. Effects of hypercaloric diet and pharmacological inhibition of casein kinase II on NFκB and NLRP3 inflammasome cascades, as well as AMPK phosphorylation in the liver. Western blot analysis of (A) IκBα phosphorylated on $Ser^{32/36}$ normalized to IκBα; (B) NFκB p65 subunit expression at nuclear and cytosolic levels; (C) NLRP3 inflammasome expression; (D) cleaved caspase-1 and total caspase-1 expression; and (E) AMPK phosphorylated on Thr^{172} and total AMPK. Densitometric analysis of the bands is presented as relative O.D. Data are presented as the mean ± SEM (n=4-5 mice/group). Statistical analysis was performed by one-way ANOVA followed by Bonferroni's post hoc test. *P<0.05 vs. SD; •P<0.05 vs. HFHS. HFHS, high-fat high-sugar; inhibitor of κB α; NLRP3, nucleotide-binding domain, leucine-rich-containing family, pyrin domain-containing-3; O.D., optical density; PCNA, proliferating cell nuclear antigen; SD, standard diet; TBB, 4,5,6,7-tetrabromobenzotriazole.

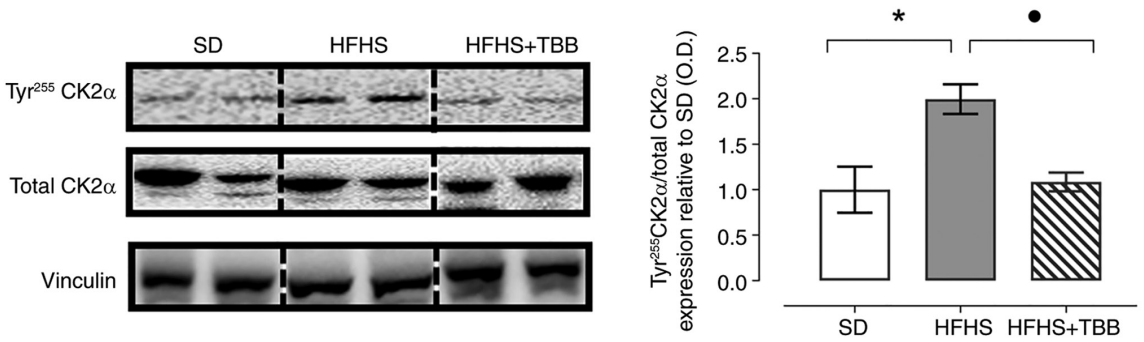

Figure 4. Effects of HFHS chronic consumption and TBB administration on CK2 activity and expression. Western blot analysis of CK2α phosphorylation on Tyr^{255} normalized to CK2α. Densitometric analysis of the bands is presented as relative O.D. Data are presented as the mean ± SEM (n=4-5 mice/group). Statistical analysis was performed by one-way ANOVA followed by Bonferroni's post hoc test. *P<0.05 vs. SD; •P<0.05 vs. HFHS. CK2, casein kinase II; O.D., optical density; HFHS, high-fat high-sugar; SD, standard diet; TBB, 4,5,6,7-tetrabromobenzotriazole.

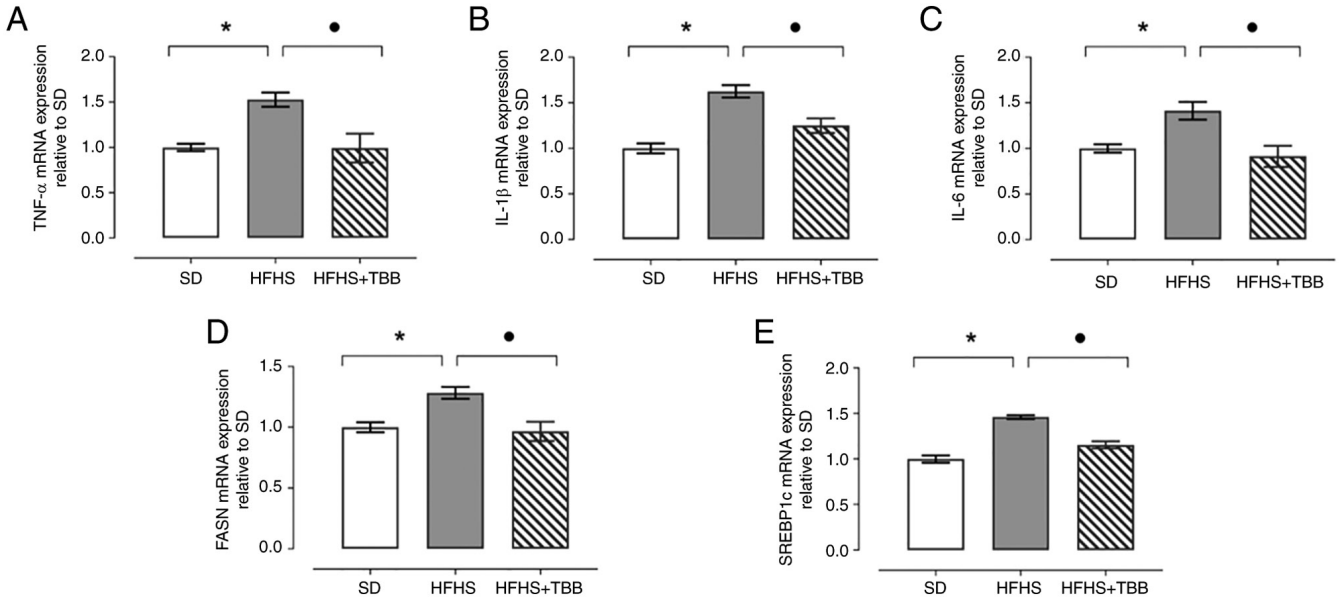

Figure 5. Assessment of hepatic pro-inflammatory and lipogenic transcript levels following dietary challenges and casein kinase II inhibition. Quantitative PCR was performed for the following genes: (A) TNF-α, (B) IL-1β, (C) IL-6, (D) FASN and (E) SREBP1c. Relative gene expression was obtained after normalization to GAPDH or 18S genes, using the formula $2^{-\Delta\Delta Cq}$ and fold change was determined by comparison to the SD group. Data are presented as the mean ± SEM (n=5-6 mice/group). Statistical analysis was performed by Kruskal-Wallis followed by Dunn's post hoc test for TNF-α and IL-6, whereas IL-1β, FASN and SREBP1c were analyzed by one-way ANOVA followed by Bonferroni's post hoc test, *P<0.05 vs. SD; •P<0.05 vs. HFHS. FASN, fatty acid nuclear synthase; HFHS, high-fat high-sugar; SD, standard diet; SREBP1c, sterol regulatory element-binding protein 1c; TBB, 4,5,6,7-tetrabromobenzotriazole.

as in p65 nuclear translocation, indicating that CK2 may be an important mediator of NFκB activation. Similarly, the HFHS diet evoked a statistically significant increased expression of the NLRP3 inflammasome and cleavage of caspase-1 in the liver homogenates of mice when compared with those in the SD-fed mice (Fig. 3C and D). Notably, TBB administration resulted in a statistically significant reduction in the expression of both NLRP3 and cleaved caspase-1. Chronic exposure to the HFHS diet markedly disrupted the phosphorylation of AMPK, a critical energy sensor, when compared with SD-fed mice, thus suggesting potential dysregulation of metabolic pathways (Fig. 3E). Notably, pharmacological intervention with TBB effectively restored basal levels of Thr^{172}AMPK phosphorylation, reversing the deleterious effects of the HFHS diet.

TBB inhibits CK2α catalytic subunit overactivation in the liver of HFHS diet-fed mice. As shown in Fig. 4, neither the hypercaloric diet nor the drug treatment evoked marked changes in the total expression of the pharmacological target of TBB, the enzyme CK2. However, the HFHS group displayed a two-fold increase in the phosphorylation of CK2α on Tyr^{255}, thus indicating an overactivation of the kinase. As expected, TBB administration significantly reduced the degree of Tyr^{255} phosphorylation of the CK2α subunit, thus confirming the ability of TBB to effectively inhibit the activity of its pharmacological target.

TBB administration mitigates local and systemic cytokine release during chronic consumption of a HFHS diet, and affects markers of hepatic lipogenesis. As shown in Fig. 5A-C, a significant increase in the mRNA expression levels of the cytokines TNF-α, IL-1β and IL-6 was recorded in the liver of HFHS diet-fed mice when compared with those in SD-fed mice. By contrast, TBB administration was associated with a marked reduction in the transcript levels of these cytokine

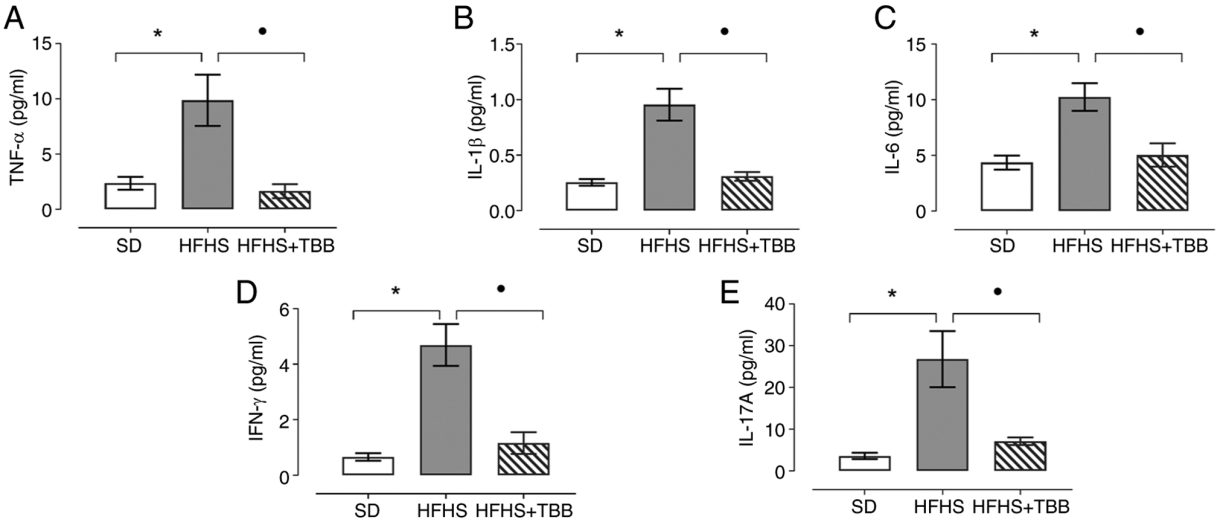

Figure 6. Effects of HFHS consumption and casein kinase II inhibition on systemic cytokine release. Plasma levels of pro-inflammatory cytokines (A) TNF-α, (B) IL-1β, (C) IL-6, (D) IFN-γ and (E) IL-17A were determined using Luminex suspension bead-based multiplexed Bio-Plex Pro™ Mouse Cytokine Th17 Panel A 6-Plex assay. Data are presented as the mean ± SEM (n=6-8 mice/group). TNF-α and IL-1β were analyzed by Kruskal-Wallis followed by Dunn's post hoc test, whereas IL-6, IFN-γ and IL-17A were analyzed by one-way ANOVA followed by Bonferroni's post hoc test, *P<0.05 vs. SD; •P<0.05 vs. HFHS. HFHS, high-fat high-sugar; SD, standard diet; TBB, 4,5,6,7-tetrabromobenzotriazole.

within the liver of mice chronically exposed to the HFHS diet. Notably, a parallelism between local levels of mRNA expression and systemic concentrations of cytokines was detected. Chronic HFHS diet intake resulted in a notable increase in the blood concentrations of several cytokines, including those detected within the liver, and also IFN-γ and IL-17A when compared with those in SD-fed mice (Fig. 6A-E). In keeping with the results obtained from liver homogenates, the administration of the CK2 inhibitor TBB resulted in the plasma cytokine levels returning to values similar to those recorded in the SD-fed mice. Moreover, HFHS diet feeding resulted in an increase in the mRNA expression levels of FASN and SREBP1c in the liver compared with those in the SD group (Fig. 5D and E), suggestive of impaired hepatic lipogenesis. Notably, TBB effectively reduced the expression levels of these two key transcription factors regulating the expression of genes related to lipid homeostasis.

Discussion

Previous studies have demonstrated that there is a causative relationship between the exposure to diets enriched in fat and sugar and the development of a low-grade chronic inflammatory response, known as metaflammation, which in turn contributes to the development of IR and related metabolic dysfunction (2,4). The insulin signaling cascade can be affected by inflammatory cytokine pathways, promoting an alteration in glucose uptake and imbalanced lipolysis, ultimately triggering ectopic lipid storage and disrupting insulin sensitivity (51). Numerous studies have identified the overactivation of inflammatory signaling cascades, including NFκB, NLRP3 inflammasome, BTK and JAK, as a result of high-fat diet feeding in mice, supporting the hypothesis that their pharmacological modulation could alleviate diet-induced abnormalities (10,11,34,52-54). However, pharmacological approaches aimed at inhibiting individual pathways show limited clinical effectiveness due to the redundancy of inflammatory cascades leading to metaflammation, and the complex interplay among various innate and adaptive immune cells altered by dietary manipulation. Therefore, the identification of crucial regulators that can specifically modulate the activation status of multiple inflammatory mediators simultaneously may represent a more effective strategy for counteracting the adverse consequences of metaflammation.

One of the main molecular patterns that serve an important role in orchestrating downstream signals perceived from the cell surface is the protein kinase family (9). Among them, CK2 is one of the first kinases that has been identified as a common modulator of several cellular processes (12,13). For example, CK2 selectively controls the activity of interdependent mediators recruited in response to inflammation, including NFκB and JAK2, and has been established to be involved in various pathological disorders associated with pro-inflammatory status (35,55). As documented in the present study, chronic exposure to a hypercaloric diet was associated with increased phosphorylation and hence overactivation of the CK2 catalytic subunit α in the mouse liver. The present findings are in agreement with those of previous studies showing the role of CK2 in pathological conditions associated with the obesogenic environment. Specifically, CK2 has been identified as a central modulator of glucose homeostasis in adipocytes and the preclinical outcomes of CK2 upregulation have been confirmed in patients affected by multiple symmetric lipomatosis, a pathological condition that includes adipose tissue expansion in its morphological phenotype (22,24). These findings are consistent with the role of CK2 in regulating thermogenesis in adipocytes (21) and in promoting pre-adipocyte differentiation, both of which contribute to the amelioration of lipid accumulation under conditions of chronic lipid overload *in vitro* and *in vivo* (23). In addition, an impairment in CK2 activity has been recorded in cardiomyocytes from insulin-resistant rats (56), highlighting the broad physiological relevance of this kinase across multiple organs. Although

CK2 has been shown to be upregulated in both abdominal visceral and subcutaneous adipose tissue from obese and obese/diabetic subjects (22), to the best of our knowledge, no data are currently available on CK2 expression or activity in the liver of these patients. Therefore, future studies involving human liver samples are warranted to validate the relevance of hepatic CK2 activation in obesity and diet-related metabolic impairments.

The present study documented that chronic exposure to a hypercaloric diet evoked a marked increase in CK2 activity in the mouse liver, without inducing relevant upregulation of CK2 expression. Notably, TBB administration resulted in a robust inhibition of CK2 activation, thus confirming its effectiveness as a CK2 inhibitor *in vivo* and its direct impact on modulating inflammation and metabolic parameters, not only at the systemic level but also directly in the liver. These beneficial effects were associated with a slight but not significant reduction in food intake and body weight, indicating that the pharmacological intervention did not exert a robust impact on mass accumulation in the present study. Notably, a recent study (23) showed significant differences in body weight gain and food intake measured in mice exposed to a hypercaloric diet in the presence or absence of high doses of a CK2 inhibitor, thus highlighting how subtle differences in the experimental protocol, as well as in drug selectivity, dosage and route of administration, can critically affect outcomes related to whole-body metabolic homeostasis.

The present results clearly demonstrated that the beneficial effects of CK2 inhibition were due, at least in part, to a significant reduction in the development of the diet-induced metaflammation. TBB treatment resulted in lower blood levels of pro-inflammatory cytokines when compared with mice exposed to the hypercaloric diet. The systemic increase in cytokines levels in response to the HFHS diet was also paralleled by an increase in leukocyte infiltration/activation in the liver, as suggested by marked increases in the local expression of the adhesion molecule ICAM-1 and cytokines (TNFα, IL-1β and IL-6), and in MPO expression and activity. These detrimental effects were efficaciously inhibited by TBB administration. The present findings are consistent with previously published data showing similar protective effects on the same markers of inflammatory response in response to another ATP-competitive CK2 inhibitor, CX-4945, which is currently under clinical investigation (57-62). This convergence of data supports the hypothesis that the protective actions observed in response to TBB may be reflective of a broader class effect of CK2 inhibition.

To identify the molecular mechanisms underlying these beneficial effects the current study focused on the cross-talk between CK2 and selective pro-inflammatory cascades, namely NFκB and NLRP3 inflammasome, the interactions of which with CK2 have been previously documented in other preclinical contexts (35,60,63). The present findings demonstrated that TBB effectively inhibited hepatic IκBα phosphorylation and prevented nuclear translocation of the NFκB p65 subunit. Given that CK2 has been shown to activate the NFκB pathway via direct phosphorylation of the IκB C-terminus and p65 subunit (14,18,19), it is plausible that the observed suppression of NFκB signaling is a direct result of local CK2 inhibition. In agreement with previous studies (62,64), the present study also documented a significant effect of the pharmacological inhibition of CK2 on diet-induced impairment of AMPK phosphorylation. Since AMPK activation has been shown to interfere with p65 nuclear translocation (65), these findings suggested that changes in AMPK phosphorylation due to TBB exposure may further contribute to the recorded down-regulation of NFκB activity in the TBB experimental group. Regarding the NLRP3 inflammasome, the protective effects of TBB likely occur via upstream inhibition of NFκB, which is a key regulator of NLRP3 expression (66) The lack of a direct impact of CK2 activity on NLRP3 inflammasome has been shown by a previous study demonstrating that CK2 activation does not result in an efficient direct control of NLRP3 phosphorylation (67). Nevertheless, in the same study, a reduction in the production of IL-1β and in the formation of ASC specks was demonstrated following CK2 knockdown, thus suggesting a functional cross-talk between CK2 and the NLRP3 inflammasome, likely involving intermediary signaling components. Overall, to the best of our knowledge, the present findings are the first to show that the pharmacological inhibition of CK2 may mitigate metaflammation by targeting critical inflammatory pathways in the liver, thereby limiting the progression of the diet-induced metabolic dysfunction.

Further mechanisms may contribute to the protection evoked by CK2 inhibition, including selective interference with signaling cascades associated with glucose homeostasis processes. For example, Pack *et al* (68) highlighted the role of CK2 in the gluconeogenesis process, due to selective modulation of the enzyme fructose-1,6-biphosphatase (FBP1). Acute administration of a CK2 inhibitor was shown to result in reduced FBP1 protein expression and activity in both *in vitro* and *in vivo* conditions, and this effect was associated with improved systemic glucose profile. CK2 has also been suggested to regulate the activity of lipogenic enzymes involved in the lipid biosynthesis. For example, CK2 indirectly modulates the activity of SREBP1 and SREPB2, which are crucial transcriptional factors for fatty acids and cholesterol synthesis (69). Specifically, CK2 activation results in an increased activity of mammalian target of rapamycin complex 1, which in turns evokes an increased SREBP1 nuclear translocation and the subsequent transcription of genes associated with lipogenesis (70). On the other hand, CK2 inhibits the activation of a negative regulator of SREBP1 nuclear translocation, namely the protein phosphatidic acid phosphatase lipin 1 (LPIN1) (71). Thus, the pharmacological inhibition of CK2 fosters LPIN1 activity, promoting the consequent reduction of SREBP1 nuclear translocation. In addition, CK2 has been shown to regulate the transcriptional activation of FASN, in response to insulin, in obese mice (72). Notably, CK2 sustains biosynthesis of desaturated lipids in renal carcinoma cells, suggesting an important role for lipid metabolism even in aberrant conditions, such as cancer (73). The present results further corroborate the involvement of CK2 in the regulation of lipogenic genes and, most notably, showed that CK2 inhibition was associated with improved transcriptional control of these genes, thus confirming the relevance of CK2 pharmacological targeting in the governance and interplay of several metabolic cascades, including lipogenesis.

Despite these compelling findings, it is important to acknowledge that additional mechanisms may contribute to the beneficial effects of TBB observed in the current study.

Although TBB is a selective ATP-competitive inhibitor of CK2, it has been reported to interfere with a limited number of other kinases, most of which are involved in oncogenic signaling pathways and are, therefore, of limited relevance in the context of the present experimental model (74). However, TBB has also been shown to inhibit glycogen synthase kinase 3 and phosphorylase kinase, two key enzymes involved in glycogenesis and glycogenolysis, respectively (75). As such, the possibility that these off-target effects may partially contribute to the improvements in blood glucose levels observed following TBB administration cannot be ruled out.

In conclusion, the present study confirmed the beneficial effects of CK2 inhibition on a murine model of diet-induced metabolic dysfunction, focusing mainly on the protective impact of TBB in blunting the hepatic inflammatory response, due to its ability to interfere with selective inflammatory pathways. These effects may contribute, at least in part, to the amelioration of the systemic glucose and lipid profiles. As previously reported, CK2 serves a pivotal role in regulating adipose tissue differentiation and activation. Therefore, the effects of TBB on adipose tissue inflammation, a key contributor to systemic metabolic dysfunction, while not examined in the present study, may represent an additional crucial mechanism underlying its protective effects. Furthermore, the potential off-target effects of TBB on other kinases or signaling pathways involved in glucose and lipid homeostasis cannot be excluded. Consequently, further studies employing more selective CK2 inhibitors, recently developed and now under clinical investigation for cancer, will be critical to better elucidate the role of CK2 in the pathophysiology of metabolic disorders and to assess the translational potential of its pharmacological modulation in this context.

Acknowledgements

Not applicable.

Funding

This work has received funding from the Italian Ministry for University and Research in the framework of the 2022 Program for Research Projects of National Interest (PRIN; grant no. 20224PR8HE).

Availability of data and materials

The data generated in the present study may be requested from the corresponding author.

Authors' contributions

EP and EA conceptualized the study and analyzed the data, performed the investigation, the visualization and validation, and designed the methodology; they wrote the original draft, reviewed and edited the manuscript. GE, GFA, DC, EM, LC, CR and RM performed the investigation, visualization and data validation. NI, MA, CC and MC conceptualized the study, and wrote, reviewed and edited the manuscript. They were also responsible for the funding acquisition and the supervision. . EP and MC confirm the authenticity of all the raw data. All authors have read and approved the final version of the manuscript.

Ethics approval and consent to participate

The *in vivo* experimental procedures performed in the present study were approved by the local Animal Use and Care Committee (University of Turin, Turin, Italy) and the Ministry of Health (approval no. 855/2021-PR).

Patient consent for publication

Not applicable.

Competing interests

The authors declare that they have no competing interests.

References

1. Budreviciute A, Damiati S, Sabir DK, Onder K, Schuller-Goetzburg P, Plakys G, Katileviciute A, Khoja S and Kodzius R: Management and prevention strategies for non-communicable diseases (NCDs) and their risk factors. Front Public Health 8: 574111, 2020.
2. Christ A and Latz E: The western lifestyle has lasting effects on metaflammation. Nat Rev Immunol 19: 267-268, 2019.
3. Malesza IJ, Malesza M, Walkowiak J, Mussin N, Walkowiak D, Aringazina R, Bartkowiak-Wieczorek J and Mądry E: High-fat, western-style diet, systemic inflammation, and gut microbiota: A narrative review. Cells 10: 3164, 2021.
4. Hotamisligil GS: Inflammation, metaflammation and immunometabolic disorders. Nature 542: 177-185, 2017.
5. Ramos-Lopez O, Martinez-Urbistondo D, Vargas-Nuñez JA and Martinez JA: The role of nutrition on meta-inflammation: Insights and potential targets in communicable and chronic disease management. Curr Obes Rep 11: 305-335, 2022.
6. van de Vyver M: Immunology of chronic low-grade inflammation: Relationship with metabolic function. J Endocrinol 257: e220271, 2023.
7. Lee YS and Olefsky J: Chronic tissue inflammation and metabolic disease. Genes Dev 35: 307-328, 2021.
8. Caputo T, Gilardi F and Desvergne B: From chronic overnutrition to metaflammation and insulin resistance: Adipose tissue and liver contributions. FEBS Lett 591: 3061-3088, 2017.
9. Nandipati KC, Subramanian S and Agrawal DK: Protein kinases: Mechanisms and downstream targets in inflammation-mediated obesity and insulin resistance. Mol Cell Biochem 426: 27-45, 2017.
10. Collotta D, Hull W, Mastrocola R, Chiazza F, Cento AS, Murphy C, Verta R, Alves GF, Gaudioso G, Fava F, *et al*: Baricitinib counteracts metaflammation, thus protecting against diet-induced metabolic abnormalities in mice. Mol Metab 39: 101009, 2020.
11. Bako HY, Ibrahim MA, Isah MS and Ibrahim S: Inhibition of JAK-STAT and NF-κB signalling systems could be a novel therapeutic target against insulin resistance and type 2 diabetes. Life Sci 239: 117045, 2019.
12. Borgo C, D'Amore C, Sarno S, Salvi M and Ruzzene M: Protein kinase CK2: A potential therapeutic target for diverse human diseases. Signal Transduct Target Ther 6: 183, 2021.
13. Roffey SE and Litchfield DW: CK2 regulation: Perspectives in 2021. Biomedicines 9: 1361, 2021.
14. Barroga CF, Stevenson JK, Schwarz EM and Verma IM: Constitutive phosphorylation of IκBα by casein kinase II (NF-κB/Rel/transcription/PEST/protein purification). Proc Natl Acad 92: 7637-7641, 1995.
15. McElhinny JA, Trushin SA, Bren GD, Chester N and Paya CV: Casein kinase II phosphorylates I kappa B alpha at S-283, S-289, S-293, and T-291 and is required for its degradation. Mol Cell Biol 16: 899-906, 1996.
16. Lin R, Beauparlant P, Makris C, Meloche S and Hiscott J: Phosphorylation of IkappaBalpha in the C-terminal PEST domain by casein kinase II affects intrinsic protein stability. Mol Cell Biol 16: 1401-1409, 1996.

17. Heilker R, Freuler F, Pulfer R, Di Padova F and Eder J: All three IkappaB isoforms and most Rel family members are stably associated with the IkappaB kinase 1/2 complex. Eur J Biochem 259: 253-261, 1999.
18. Chantôme A, Pance A, Gauthier N, Vandroux D, Chenu J, Solary E, Jeannin JF and Reveneau S: Casein kinase II-mediated phosphorylation of NF-kappaB p65 subunit enhances inducible nitric-oxide synthase gene transcription in vivo. J Biol Chem 279: 23953-23960, 2004.
19. Manni S, Brancalion A, Mandato E, Tubi LQ, Colpo A, Pizzi M, Cappellesso R, Zaffino F, Di Maggio SA, Cabrelle A, *et al*: Protein kinase CK2 inhibition down modulates the NF-κB and STAT3 survival pathways, enhances the cellular proteotoxic stress and synergistically boosts the cytotoxic effect of bortezomib on multiple myeloma and mantle cell lymphoma cells. PLoS One 8: e75280, 2013.
20. Lan YC, Wang YH, Chen HH, Lo SF, Chen SY and Tsai FJ: Effects of casein kinase 2 alpha 1 gene expression on mice liver susceptible to type 2 diabetes mellitus and obesity. Int J Med Sci 17: 13-20, 2020.
21. Shinoda K, Ohyama K, Hasegawa Y, Chang HY, Ogura M, Sato A, Hong H, Hosono T, Sharp LZ, Scheel DW, *et al*: Phosphoproteomics identifies CK2 as a negative regulator of beige adipocyte thermogenesis and energy expenditure. Cell Metab 22: 997-1008, 2015.
22. Borgo C, Milan G, Favaretto F, Stasi F, Fabris R, Salizzato V, Cesaro L, Belligoli A, Sanna M, Foletto M, *et al*: CK2 modulates adipocyte insulin-signaling and is up-regulated in human obesity. Sci Rep 7: 17569, 2017.
23. Buchwald LM, Neess D, Hansen D, Doktor TK, Ramesh V, Steffensen LB, Blagoev B, Litchfield DW, Andresen BS, Ravnskjaer K, *et al*: Body weight control via protein kinase CK2: Diet-induced obesity counteracted by pharmacological targeting. Metabolism 162: 156060, 2025.
24. Sanna M, Borgo C, Compagnin C, Favaretto F, Vindigni V, Trento M, Bettini S, Comin A, Belligoli A, Rugge M, *et al*: White adipose tissue expansion in multiple symmetric lipomatosis is associated with upregulation of CK2, AKT and ERK1/2. Int J Mol Sci 21: 7933, 2020.
25. Chen Y, Varghese Z and Ruan XZ: The molecular pathogenic role of inflammatory stress in dysregulation of lipid homeostasis and hepatic steatosis. Genes Dis 1: 106-112, 2014.
26. Ke B, Zhao Z, Ye X, Gao Z, Manganiello V, Wu B and Ye J: Inactivation of NF-κB p65 (RelA) in liver improves insulin sensitivity and inhibits cAMP/PKA pathway. Diabetes 64: 3355-3362, 2015.
27. Cai D, Yuan M, Frantz DF, Melendez PA, Hansen L, Lee J and Shoelson SE: Local and systemic insulin resistance resulting from hepatic activation of IKK-beta and NF-kappaB. Nat Med 11: 183-190, 2005.
28. Huang H, Lee SH, Sousa-Lima I, Kim SS, Hwang WM, Dagon Y, Yang WM, Cho S, Kang MC, Seo JA, *et al*: Rho-kinase/AMPK axis regulates hepatic lipogenesis during overnutrition. J Clin Invest 128: 5335-5350, 2018.
29. Percie du Sert N, Ahluwalia A, Alam S, Avey MT, Baker M, Browne WJ, Clark A, Cuthill IC, Dirnagl U, Emerson M, *et al*: Reporting animal research: Explanation and elaboration for the ARRIVE guidelines 2.0. PLoS Biol 18: e3000411, 2020.
30. Directive 2010/63/EU of the European parliament and of the council of 22 september 2010 on the protection of animals used for scientific purposes (Text with EEA relevance), 2010.
31. National Research Council (US) Committee for the Update of the Guide for the Care and Use of Laboratory Animals: Guide for the Care and Use of Laboratory Animals. 8th edition. National Academies Press (US), Washington, DC, 2011.
32. Collino M, Mastrocola R, Nigro D, Chiazza F, Aragno M, D'Antona G and Minetto MA: Variability in myosteatosis and insulin resistance induced by high-fat diet in mouse skeletal muscles. Biomed Res Int 2014: 569623, 2014.
33. Xia B, Zhu R, Zhang H, Chen B, Liu Y, Dai X, Ye Z, Zhao D, Mo F, Gao S, *et al*: Lycopene improves bone quality and regulates AGE/RAGE/NF-κB signaling pathway in high-fat diet-induced obese mice. Oxid Med Cell Longev 2022: 3697067, 2022.
34. Chiazza F, Couturier-Maillard A, Benetti E, Mastrocola R, Nigro D, Cutrin JC, Serpe L, Aragno M, Fantozzi R, Ryffel B, *et al*: Targeting the NLRP3 inflammasome to reduce diet-induced metabolic abnormalities in mice. Mol Med 21: 1025-1037, 2015.
35. Huang J, Chen Z, Li J, Chen Q, Li J, Gong W, Huang J, Liu P and Huang H: Protein kinase CK2α catalytic subunit ameliorates diabetic renal inflammatory fibrosis via NF-κB signaling pathway. Biochem Pharmacol 132: 102-117, 2017.
36. Chen Z, Chen Q, Huang J, Gong W, Zou Y, Zhang L, Liu P and Huang H: CK2α promotes advanced glycation end products-induced expressions of fibronectin and intercellular adhesion molecule-1 via activating MRTF-A in glomerular mesangial cells. Biochem Pharmacol 148: 41-51, 2018.
37. Brehme H, Kirschstein T, Schulz R and Köhling R: In vivo treatment with the casein kinase 2 inhibitor 4,5,6,7-tetrabromotriazole augments the slow afterhyperpolarizing potential and prevents acute epileptiform activity. Epilepsia 55: 175-183, 2014.
38. National Centre for the Replacement Refinement and Reduction of Aninals in Research: Microsampling. https://nc3rs.org.uk/3rs-resources/microsampling#microsampling-study-designs. Accessed June 17, 2025.
39. National Institutes of Health (NIH), Animal Research Advisory Committee (ARAC), National Institutes of Health (NIH) and Animal Research Advisory Committee (ARAC): Guidelines for Survival Blood Collection in Mice and Rats. https://oacu.oir.nih.gov/system/files/media/file/2022-12/b2-Survival_Blood_Collection_Mice_Rats.pdf. Accessed June 17, 2025.
40. University of Kentucky: Guidelines for Blood Collection in Laboratory Animals. https://research.uky.edu/division-laboratory-animal-resources/guidelines-blood-collection-laboratory-animals. Accessed June 17, 2025.
41. Swiss Animal Welfare Officer Network (AWON): Guideline on blood collection techniques in rodents and rabbits. https://portal-cdn.scnat.ch/asset/aa5ba763-49be-5603-b964-c59d0cbd932f/AWON%20Blood%20coll%20Guideline%20Final%20Publ.pdf?b=eb714836-a777-530c-89db-69ff16d3774e&v=313fdd66-5ae2-5085-8364-bd2045117053_0&s=Mf4vKYyAmFEoqPTJTfB7z0RwOdBNqZWEXv_XpVGu6jl8wJ0B_Mjy-0ga8ZrOJX0zLnOPTg1yKb7h9Gh9Cx_oLPBsZ9Taub11Xb7QSBMar0KPHPp59VkUMj99iiOCdRDeZ124RZBfS0ceD0IuZLR6SNV6S2El4DGP-d-AIomqFEQ. Accessed June 17, 2025.
42. O'Donnell KL, Knopick PL, Larsen R, Sarkar S, Nilles ML and Bradley DS: Difference in strain pathogenicity of septicemic yersinia pestis infection in a TLR2$^{-/-}$ mouse model. Infect Immun 88: e00792-19, 2020.
43. Kovalski V, Prestes AP, Oliveira JG, Alves GF, Colarites DF, Mattos JE, Sordi R, Vellosa JC and Fernandes D: Protective role of cGMP in early sepsis. Eur J Pharmacol 807: 174-181, 2017.
44. Aimaretti E, Porchietto E, Mantegazza G, Gargari G, Collotta D, Einaudi G, Ferreira Alves G, Marzani E, Algeri A, Dal Bello F, *et al*: Anti-glycation properties of zinc-enriched Arthrospira platensis (spirulina) contribute to prevention of metaflammation in a diet-induced obese mouse model. Nutrients 16: 552, 2024.
45. Fornelli C, Sofia Cento A, Nevi L, Mastrocola R, Ferreira Alves G, Caretti G, Collino M and Penna F: The BET inhibitor JQ1 targets fat metabolism and counteracts obesity. J Adv Res 68: 403-413, 2025.
46. Jiang L, Wang Q, Yu Y, Zhao F, Huang P, Zeng R, Qi RZ, Li W and Liu Y: Leptin contributes to the adaptive responses of mice to high-fat diet intake through suppressing the lipogenic pathway. PLoS One 4: e6884, 2009.
47. Serino M, Luche E, Gres S, Baylac A, Bergé M, Cenac C, Waget A, Klopp P, Iacovoni J, Klopp C, *et al*: Metabolic adaptation to a high-fat diet is associated with a change in the gut microbiota. Gut 61: 543-553, 2012.
48. Lo YH, Ho PC, Chen MS, Hugo E, Ben-Jonathan N and Wang SC: Phosphorylation at tyrosine 114 of proliferating cell nuclear antigen (PCNA) is required for adipogenesis in response to high fat diet. Biochem Biophys Res Commun 430: 43-48, 2013.
49. Livak KJ and Schmittgen TD: Analysis of relative gene expression data using real-time quantitative PCR and the 2(-Delta Delta C(T)) method. Methods 25: 402-408, 2001.
50. Yu H, Liu Y, Wang M, Restrepo RJ, Wang D, Kalogeris TJ, Neumann WL, Ford DA and Korthuis RJ: Myeloperoxidase instigates proinflammatory responses in a cecal ligation and puncture rat model of sepsis. Am J Physiol Heart Circ Physiol 319: H705-H721, 2020.
51. Schleh MW, Caslin HL, Garcia JN, Mashayekhi M, Srivastava G, Bradley AB and Hasty AH: Metaflammation in obesity and its therapeutic targeting. Sci Transl Med 15: eadf9382, 2023.
52. Vandanmagsar B, Youm YH, Ravussin A, Galgani JE, Stadler K, Mynatt RL, Ravussin E, Stephens JM and Dixit VD: The NLRP3 inflammasome instigates obesity-induced inflammation and insulin resistance. Nat Med 17: 179-188, 2011.

53. Purvis GSD, Collino M, Aranda-Tavio H, Chiazza F, O'Riordan CE, Zeboudj L, Mohammad S, Collotta D, Verta R, Guisot NES, *et al*: Inhibition of Bruton's TK regulates macrophage NF-κB and NLRP3 inflammasome activation in metabolic inflammation. Br J Pharmacol 177: 4416-4432, 2020.
54. Li Y, Zhao J, Wu Y and Xia L: Btk knockout attenuates the liver inflammation in STZ-induced diabetic mice by suppressing NLRP3 inflammasome activation. Biochem Biophys Res Commun 549: 75-82, 2021.
55. Yamada M, Katsuma S, Adachi T, Hirasawa A, Shiojima S, Kadowaki T, Okuno Y, Koshimizu TA, Fujii S, Sekiya Y, *et al*: Inhibition of protein kinase CK2 prevents the progression of glomerulonephritis. Proc Natl Acad Sci USA 102: 7736-7741, 2005.
56. Durak A, Bitirim CV and Turan B: Titin and CK2α are new intracellular targets in acute insulin application-associated benefits on electrophysiological parameters of left ventricular cardiomyocytes from insulin-resistant metabolic syndrome rats. Cardiovasc Drugs Ther 34: 487-501, 2020.
57. Drygin D, Ho CB, Omori M, Bliesath J, Proffitt C, Rice R, Siddiqui-Jain A, O'Brien S, Padgett C, Lim JK, *et al*: Protein kinase CK2 modulates IL-6 expression in inflammatory breast cancer. Biochem Biophys Res Commun 415: 163-167, 2011.
58. Ye H, Fu D, Fang X, Xie Y, Zheng X, Fan W, Hu F and Li Z: Casein kinase II exacerbates rheumatoid arthritis via promoting Th1 and Th17 cell inflammatory responses. Expert Opin Ther Targets 25: 1017-1024, 2021.
59. Huang W, Zheng X, Huang Q, Weng D, Yao S, Zhou C, Li Q, Hu Y, Xu W and Huang K: Protein kinase CK2 promotes proliferation, abnormal differentiation, and proinflammatory cytokine production of keratinocytes via regulation of STAT3 and Akt pathways in psoriasis. Am J Pathol 193: 567-578, 2023.
60. Ferreira Alves G, Aimaretti E, da Silveira Hahmeyer ML, Einaudi G, Porchietto E, Rubeo C, Marzani E, Aragno M, da Silva-Santos JE, Cifani C, *et al*: Pharmacological inhibition of CK2 by silmitasertib mitigates sepsis-induced circulatory collapse, thus improving septic outcomes in mice. Biomed Pharmacother 178: 117191, 2024.
61. Ampofo E, Rudzitis-Auth J, Dahmke IN, Rössler OG, Thiel G, Montenarh M, Menger MD and Laschke MW: Inhibition of protein kinase CK2 suppresses tumor necrosis factor (TNF)-α-induced leukocyte-endothelial cell interaction. Biochim Biophys Acta 1852: 2123-2136, 2015.
62. Yadav AK and Jang BC: Anti-adipogenic and pro-lipolytic effects on 3T3-L1 preadipocytes by CX-4945, an inhibitor of casein kinase 2. Int J Mol Sci 23: 7274, 2022.
63. Ka SO, Hwang HP, Jang JH, Hyuk Bang I, Bae UJ, Yu HC, Cho BH and Park BH: The protein kinase 2 inhibitor tetrabromobenzotriazole protects against renal ischemia reperfusion injury. Sci Rep 5: 14816, 2015.
64. Dixit D, Ahmad F, Ghildiyal R, Joshi SD and Sen E: CK2 inhibition induced PDK4-AMPK axis regulates metabolic adaptation and survival responses in glioma. Exp Cell Res 344: 132-142, 2016.
65. Salminen A, Hyttinen JM and Kaarniranta K: AMP-activated protein kinase inhibits NF-κB signaling and inflammation: impact on healthspan and lifespan. J Mol Med (Berl) 89: 667-676, 2011.
66. Liu T, Zhang L, Joo D and Sun SC: NF-κB signaling in inflammation. Signal Transduct Target Ther 2: 17023, 2017.
67. Niu T, De Rosny C, Chautard S, Rey A, Patoli D, Groslambert M, Cosson C, Lagrange B, Zhang Z, Visvikis O, *et al*: NLRP3 phosphorylation in its LRR domain critically regulates inflammasome assembly. Nat Commun 12: 5862, 2021.
68. Pack M, Gulde TN, Völcker MV, Boewe AS, Wrublewsky S, Ampofo E, Montenarh M and Götz C: Protein kinase CK2 contributes to glucose homeostasis by targeting fructose-1,6-bisphosphatase 1. Int J Mol Sci 24: 428, 2022.
69. Guerra B and Issinger OG: Role of protein kinase CK2 in aberrant lipid metabolism in cancer. Pharmaceuticals (Basel) 13: 292, 2020.
70. Peterson TR, Sengupta SS, Harris TE, Carmack AE, Kang SA, Balderas E, Guertin DA, Madden KL, Carpenter AE, Finck BN and Sabatini DM: mTOR complex 1 regulates lipin 1 localization to control the SREBP pathway. Cell 146: 408-420, 2011.
71. Hennessy M, Granade ME, Hassaninasab A, Wang D, Kwiatek JM, Han GS, Harris TE and Carman GM: Casein kinase II-mediated phosphorylation of lipin 1β phosphatidate phosphatase at Ser-285 and Ser-287 regulates its interaction with 14-3-3β protein. J Biol Chem 294: 2365-2374, 2019.
72. Viscarra JA, Wang Y, Hong IH and Sul HS: Transcriptional activation of lipogenesis by insulin requires phosphorylation of MED17 by CK2. Sci Signal 10: eaai8596, 2017.
73. Guerra B, Jurcic K, van der Poel R, Cousineau SL, Doktor TK, Buchwald LM, Roffey SE, Lindegaard CA, Ferrer AZ, Siddiqui MA, *et al*: Protein kinase CK2 sustains de novo fatty acid synthesis by regulating the expression of SCD-1 in human renal cancer cells. Cancer Cell Int 24: 432, 2024.
74. Pagano MA, Bain J, Kazimierczuk Z, Sarno S, Ruzzene M, Di Maira G, Elliott M, Orzeszko A, Cozza G, Meggio F and Pinna LA: The selectivity of inhibitors of protein kinase CK2: An update. Biochem J 415: 353-365, 2008.
75. Sarno S, Reddy H, Meggio F, Ruzzene M, Davies SP, Donella-Deana A, Shugar D and Pinna LA: Selectivity of 4,5,6,7-tetrabromobenzotriazole, an ATP site-directed inhibitor of protein kinase CK2 ('casein kinase-2'). FEBS Lett 496: 44-48, 2001.